Journal of Catalysis **203,** 75–81 (2001)
doi:10.1006/jcat.2001.3319, available online at http://www.idealibrary.com on IDEAL®

Selective Oxidation of Cyclopentene to Glutaraldehyde by H_2O_2 over the WO_3/SiO_2 Catalyst

Ronghua Jin,* Hexing Li,*,[1] and Jing-Fa Deng†

*Department of Chemistry, Shanghai Normal University, Shanghai 200234, P. R. China; and †Department of Chemistry, Fudan University, Shanghai 200433, P. R. China

Received December 4, 2000; revised May 31, 2001; accepted June 14, 2001

A novel WO_3/SiO_2 was prepared by incipient wetness impregnation of the SiO_2 support synthesized by the xerogel method with the W-containing salt solution. The as-prepared WO_3/SiO_2 catalyst exhibited a very high yield of glutaraldehyde in the liquid phase cyclopentene oxidation by aqueous H_2O_2 and the leach of WO_3 species during the reaction could be neglected. As a heterogeneous catalyst, it seems more suitable for the industrial process than those homogeneous catalysts owing to its easy separation from reaction products, which makes it possible to use the catalyst repetitively. According to the XRD patterns, the WO_3 was present in amorphous state due to its high dispersion on the SiO_2 support. These amorphous WO_3 species were proved to be the active sites since the crystallization at high temperature caused a considerable deactivation. The lifetime of the catalyst was measured and its regeneration method was proposed. Effects of various factors on the catalytic behaviors, such as the WO_3 loading, the calcination temperature, and the reaction media, were also investigated and discussed based on the characterizations of BET, XRD, DSC, TEM, EXAFS, and Raman spectra.

Key Words: **WO_3/SiO_2 catalyst; selective oxidation; cyclopentene; H_2O_2; glutaraldehyde; xerogel method.**

INTRODUCTION

WO_3-based catalysts are important not only in selective reduction of NH_3 (1–3) but also in epoxidation of unsaturated compounds (4). Supported tungsten oxide catalysts are very efficient for various acid catalyzed heterogeneous reactions. However, almost no attention has been devoted to their application in the oxidative cleavage of carbon–carbon double bonds with aqueous H_2O_2 to produce dialdehydes, which is now mainly prepared by ozonization of olefins (5, 6) or other synthetic methods (7, 8). Glutaraldehyde (GA) has been used extensively for disinfection and sterilization in many areas (9). An important way to produce GA is the selective oxidative cleavage of cyclopentene (CPE), since a great quantity of CPE could be easily obtained from the byproducts of C_5 fraction presented in refining oils (10, 11). Recently, several W-containing homogeneous catalysts have been reported which allowed us to use the environmentally friendly aqueous H_2O_2 as the oxidant for the CPE selective oxidation to GA (12–14). Although the high GA yield was obtained, their application in industrial processes seems impractical since the separation of these homogeneous catalysts from the reaction products is very difficult. On one hand, product cleanup is evitable. On the other hand, the catalyst cannot be used repetitively and regenerated. One of the most promising ways is to design the W-containing heterogeneous catalysts by depositing the WO_3 species on the suitable supports. As we know, however, no such a work has been reported so far, possibly due to the poor catalytic efficiency of the heterogeneous catalysts in comparison with the corresponding homogeneous catalysts. Our previous studies demonstrated that the pore size of the support played a key role in determining the performance of the supported heterogeneous catalysts, since the large pore size of the support is necessary to ensure the oxidation of bulky cycloalkenes over those catalysts (15, 16). In the present paper, we report a novel WO_3/SiO_2 with larger pore size based on the combination of both the xerogel method and the incipient wetness impregnation. The as-prepared WO_3/SiO_2 catalyst exhibited a very high GA yield in liquid phase CPE oxidation by aqueous H_2O_2, almost the same as that obtained by using the tungstic acid as a homogeneous catalyst. The effects of various factors on its catalytic behaviors were determined and well discussed according to various characterizations.

EXPERIMENTAL

Catalyst Preparation

The SiO_2 support was prepared by an alkoxide-sol-gel method (17–20). In general, a certain amount of ethanol was added to 150 ml tetraethylsilicate (TEOS) solution. After being stirred for 30 min, water and HCl solution were added to the above solution, in which the molar ratio of H_2O : TEOS : HCl was adjusted to be

[1] To whom correspondence should be addressed. E-mail: HeXingLi@shtu.edu.cn.

0021-9517/01 $35.00

5 : 1 : 0.09. The gel was kept at 353 K for 24 h and then at 373 K for another 24 h, which resulted in a dried gel. The powder of dried support was then ground with mortar and pestle and sieved to 80–100 meshes. Then, the sample was heated programmed at 5 K/min in a nitrogen flow of 500 ml/min and kept at 473 K for 2 h. After cooling down to 353 K, it was calcined in an air flow of 500 ml/min at a programmed temperature with the speed of 5 K/min up to 823 K and kept at that temperature for another 4 h to remove most of the organic residues. The WO_3/SiO_2 was obtained by an incipient wetness impregnation of the as-prepared SiO_2 support with appropriate amounts of ammonium tungstate solution (2, 21–23), which was then dried at 393 K for 16 h following a calcination in air flow at 823 K for another 16 h.

Catalyst Characterization

Specific surface areas (BET) and mean cylindrical pore diameters were determined by nitrogen physisorption at 77 K using a Micromeritics ASAP 2000 instrument.

X-ray powder diffraction (XRD) patterns were obtained on a Bruker D8 Advance X-ray generator using Cu Kα radiation ($\lambda = 1.54$ Å) at 40 kV and 40 mA.

Differential scanning calorimetry (DSC) was conducted under nitrogen (99.99%) atmosphere on a Dupont 9900 computer-thermal analysis system at the heating rate of 10 K min^{-1}.

Transmission electron microscope (TEM) was obtained on a Hitachi H600 scan-transmission electron microscope.

Extended X-ray absorption fine structure (EXAFS) was performed. The absorption data of W *k*-edge were collected at the 4W1B beamline in Beijing Synchrotron Radiation Facility, China. The electron beam energy is 22.0 GeV and the stored current is in the range of 30–50 mA. The monochromator is a channel-cut Si(111) crystal monochromator; $d = 0.31355$ nm. The data were collected in the transmission mode using ion chambers of nitrogen (75%) argon (25%) mixed gas at room temperatures from 8050 to 9400 eV. We registered data three times for estimating the deviation. Data were processed by using the program package FXEA.

Raman spectra were recorded with a Superlab Ram Raman spectrometer with a resolution of 2 cm^{-1}. The laser power at the sample location was set to 15 mW. The excitation line of the Raman scattering was 632.817 nm.

Activity Test

In a typical run, the oxidation experiment was carried out in a sealed 10-ml glass reactor in which 0.5 ml of CPE (Fluka), 5 ml of t-BuOH (as the solvent), and 0.2 g catalyst were mixed at 308 K with vigorous stirring. The reaction was started by adding 0.7-ml 50% aqueous H_2O_2 solution (industrial grade) into the mixture and was kept for 24 h. The conversion of CPE was measured by gas chromatograph with TCD detector by using cyclopentane as an internal standard. The yield of GA was measured by gas chromatograph with FID detector by using an external standard method. The products were analyzed by GC-MS. The H_2O_2 was measured by standard iodometric titration.

RESULTS AND DISCUSSION

Comparison of Different Catalysts

The WO_3/SiO_2 catalysts with different WO_3 loadings exhibited different activities and selectivities to GA during the CPE oxidation. As shown in Table 1, the GA yield first increased rapidly with the increase of the WO_3 loadings up to 15 wt% and then kept nearly constant when the WO_3 loadings further increased, indicating the optimum WO_3 loading was 15 wt%. Although the GA yield over 15 wt% WO_3/SiO_2 catalyst was slightly lower than that on the corresponding homogeneous catalyst obtained by dissolving $WO_3 \cdot H_2O$ in the reaction solution, the WO_3/SiO_2 catalyst, as a heterogeneous catalyst, was more suitable for the industrial process since it could be used repetitively during the reaction owing to its easy separation from the reaction mixture. After reaction for three times, significant decrease in the GA yield was observed, showing the occurrence of the catalyst deactivation. Such a deactivation was possibly due to the covering of the catalyst surface with the organic species since the activity could be recovered mostly by calcining the catalyst at 823 K for 6 h.

According to the ICP analysis, only 2.3 ppm W-species was detected in the solution after reaction for 24 h with 15 wt% WO_3/SiO_2 catalyst, showing that the loss of W-species could be neglected. To make sure whether the heterogeneous WO_3 on the SiO_2 support or the dissolved homogeneous WO_3 was the real catalyst responsible for

TABLE 1

Structural Properties and Catalytic Performance of Different WO_3/SiO_2 Catalysts[a]

WO_3 loading (wt%)	BET ($m^2 \cdot g^{-1}$)	V_p (N_2) ($cm^3 \cdot g^{-1}$)	d_p (nm)	Conversion (%)		Yield (%) GA
				CPE	H_2O_2	
5	569	0.28	1.9	95.5	98.6	46.3
10	539	0.28	1.9	97.8	99.1	54.9
15	522	0.27	1.9	100	100	59.9
20	475	0.27	1.8	100	100	60.0
$WO_3 \cdot H_2O$[b]	—	—	—	100	100	62.3
WO_3[c]	—	—	—	1.5	0.1	0
15[d]	502	0.28	1.8	98.3	100	57.5

[a] Reaction conditions: 308 K, 0.2 g catalyst (calcined at 823 K), 0.5 ml CPE, 0.7 ml 50% H_2O_2, 5 ml t-BuOH, reaction for 24 h.

[b] Homogeneous catalyst.

[c] Insoluble WO_3 obtained after $WO_3 \cdot H_2O$ was calcined at 673 K.

[d] The catalyst after regeneration.

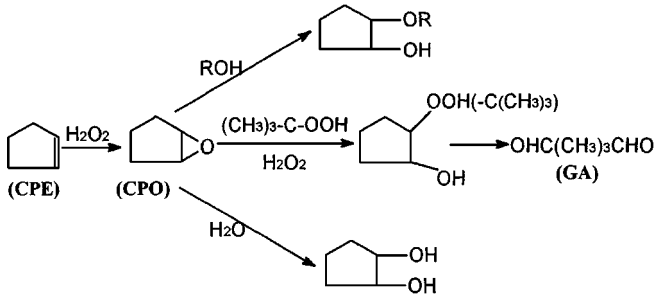

SCHEME 1. The reaction route of cyclopentene (CPE) oxidation.

the present oxidation, the following procedure, proposed by Sheldon *et al.* (24), was carried out. After reaction for 4.5 h in which the CPE conversion reached nearly 61.6%, the reaction mixture was filtered and then allowed the mother liquor (filtrate) to react for another 16 h at the same reaction conditions. No significant activity was observed, demonstrating that the active species are not the dissolved WO_3 leached from WO_3/SiO_2. Therefore it is reasonable to suggest that the present catalysis is heterogeneous in nature.

According to the GC-MS analysis, besides GA as the main product, a variety of the byproducts, such as oxide (CPO), cyclopentanone, 2-cyclopenten-1-one, *trans*-1,2-cyclopentandiol and its mono ether, were observed, indicating that the reaction was very complex. Therefore, a possible reaction scheme was described as follows (Scheme 1).

Over the 15 wt% WO_3/SiO_2 catalyst with WO_3 loading of 15 wt%, the dependence of the contents of CPE, GA, and various byproducts on the reaction time is illustrated in Fig. 1. As the CPO produced rapidly at the beginning and then consumed progressively with the increase of GA, one can conclude that CPO was possibly a main intermediate from which GA produced via its further oxidative cleavage.

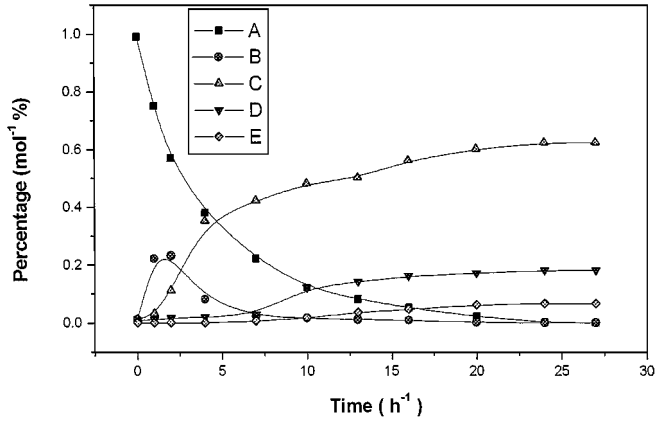

FIG. 1. Dependence of distribution of CPE and the products on the reaction time. A = CPE, B = CPO, C = GA, D = *trans*-1,2-cyclopentandiol, E = 1,2-cyclopentandiol mono ether. Reaction conditions: 308 K, 0.2 g 15 wt% WO_3/SiO_2 catalyst calcined at 823 K, 0.5 ml CPE, 0.7 ml 50% H_2O_2, 5 ml t-BuOH.

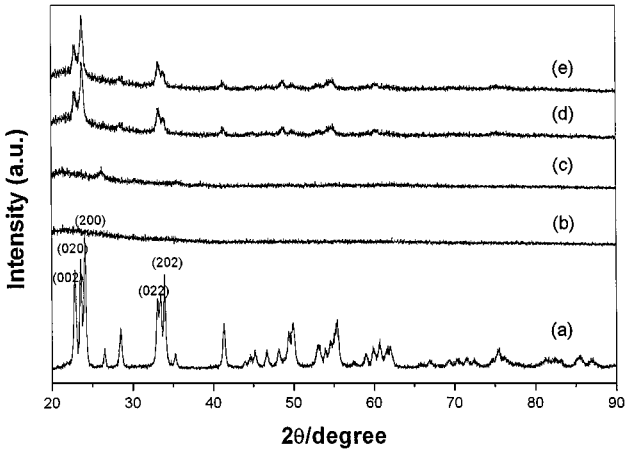

FIG. 2. XRD patterns of (a) anhydrous WO_3, and the 15% WO_3/SiO_2 sample calcined at 823 K, (b) before reaction, (c) after regeneration, (d) after reaction for three times (72 h), and (e) the 15% WO_3/SiO_2 sample calcined at 973 K.

After $WO_3 \cdot H_2O$ was calcined at 673 K for 12 h, an anhydrous WO_3 sample was obtained which is insoluble in the aqueous H_2O_2. Against expectation, almost no activity was observed over such an anhydrous WO_3 catalyst, as shown in Table 1.

The above results could be explained based on the XRD analysis. As shown in Fig. 2, the anhydrous WO_3 exhibited a typical crystalline structure while the fresh WO_3/SiO_2 exhibited a typical amorphous structure. According to the activity test, as shown in Table 1, the anhydrous WO_3 exhibited almost no activity during the reaction. Therefore, one can conclude that the WO_3 species in amorphous state were the active sites in the present catalysis. At lower WO_3 loadings (<20 wt%), the WO_3 species were well dispersed on the support surface without significant crystallization. Thus, the GA yield increased with the increase of WO_3 loadings since the number of surface active WO_3 sites increased. However, partial crystallization occurred at higher WO_3 loadings (>20 wt%), which was responsible for the decrease in its activity. The crystallization of WO_3/SiO_2 at higher WO_3 loadings was possibly due to the gathering of the WO_3 particles since the BET surface area decreased rapidly with the increase of WO_3 loadings, as shown in Table 1. After reaction for three times, GA yield decreased since partial crystalline WO_3 appeared. The activity could be recovered mostly by calcining the catalyst at 823 K for 6 h since the amorphous WO_3 species were obtained again after its regeneration.

The relationship between the crystallization of WO_3 species and its dispersion on the SiO_2 support was further illustrated by the TEM. As shown in Fig. 3a, the fresh WO_3/SiO_2 sample exhibited a well dispersed morphology comprising very small particles. These particles are spherical with an average size around 10–60 nm. After reaction for three times, big lumps with an average size larger than 100 nm appeared owing to the gathering of the WO_3

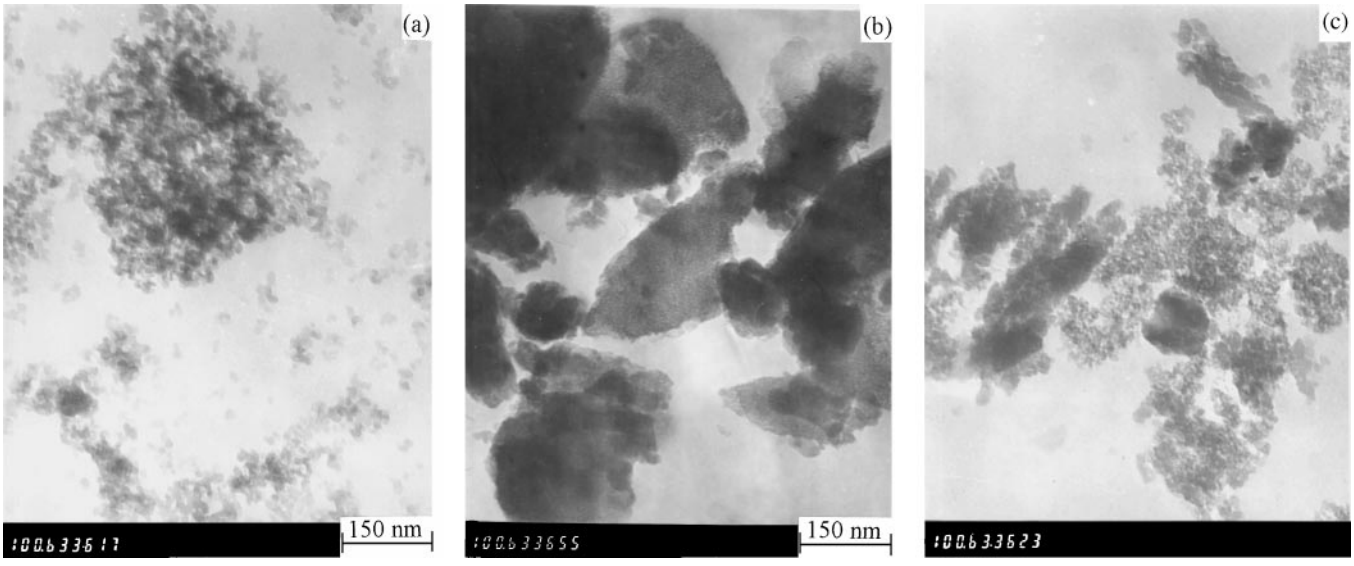

FIG. 3. TEM photograph of the as-prepared 15% WO_3/SiO_2 sample calcined at 823 K. (a) before reaction, (b) after reaction for three times (72 h), and (c) after regeneration.

particles, as shown in Fig. 3b. After the regeneration of the catalyst, these big lumps disappeared and the well-dispersed morphology similar to that in Fig. 3a appeared again (see Fig. 3c). One can see that the particle size was around 30–100 nm, which was slightly larger than that in the fresh WO_3/SiO_2 sample.

Influence of the Calcination Temperature

To further confirm the correlation of the activity of WO_3 to its structure, the *in situ* XRD patterns of 15 wt% WO_3/SiO_2 catalyst treated at elevated calcination temperatures were determined and their corresponding activity and GA yield were measured. As shown in Fig. 4, the *in situ* XRD patterns revealed that the WO_3 was present in an amorphous state on the SiO_2 support when the calcination temperature was lower than 823 K. However, when the WO_3/SiO_2 catalyst was treated at higher temperatures from 823 to 1073 K, several diffraction peaks appeared. Those peaks were assigned to the crystalline WO_3 phases since no significant diffraction peaks of SiO_2 support were observed; even it was treated at 1073 K. Considering the change of catalytic performance, as shown in Table 2, the CPE conversion remained at 100% while the GA yield increased from 41.4 to 59.9% when the calcinations temperatures increased from 673 to 823 K. However, both the activity and GA yield decreased dramatically when the calcination temperatures further increased from 823 to 1073 K. This clearly demonstrated that only the amorphous WO_3 phase could serve as the active sites during the present catalysis. The crystallization process of 15 wt% WO_3/SiO_2 sample could also be analyzed by DSC, as shown in Fig. 5. The single exothermic peak on the DSC spectra suggested that the WO_3/SiO_2 sample transferred from the amorphous state to its crystallized state at around 873 K without any

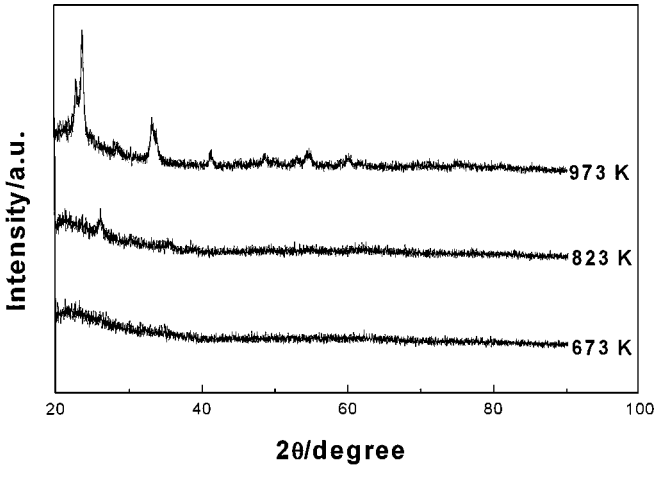

FIG. 4. *In situ* XRD patterns of 15 wt% WO_3/SiO_2 sample calcined at 673, 823, and 973 K, respectively.

TABLE 2

Influence of the Calcination Temperature on the Structural and Catalytic Properties of the WO_3/SiO_2 Catalyst with 15 wt% WO_3 Loading[a]

Temperature (K)	BET ($m^2\,g^{-1}$)	V_p (N_2) ($cm^3\,g^{-1}$)	d_p (nm)	Conversion (%) CPE	Conversion (%) H_2O_2	Yield (%) GA
673	610	0.29	1.7	100	100	41.4
823	522	0.27	1.9	100	100	59.9
973	367	0.19	2.2	48.7	52.4	19.7

[a] Reaction conditions are as the same as those given in Table 1.

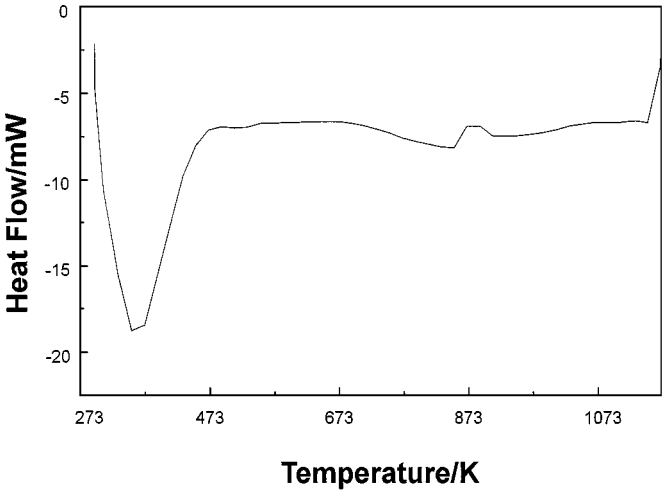

FIG. 5. DSC curve of the 15% WO_3/SiO_2 sample calcined at 823 K.

other intermediate phases. As well known, the higher calcination temperatures could increase the interaction between WO_3 and the SiO_2 support and in turn inhibit the leaching of the active WO_3 during the reaction. Therefore, 823 K was chosen as the optimum calcination temperature of 15 wt% WO_3/SiO_2 catalyst because at that temperature no significant crystallization occurred. It should be noted that the crystallization temperature changed with the WO_3 loading. Lower calcination temperatures should be employed with higher WO_3 loadings to avoid crystallization.

The Raman spectra provided additional information about the structure of the WO_3/SiO_2 samples, as shown in Fig. 6. One can see that the WO_3/SiO_2 calcined at 823 K was present in a typical amorphous state since no significant peaks appeared, as shown in Fig. 6a. After reaction for three times, various strong bands around 800, 720, and 270 cm^{-1} corresponding to the symmetric stretching mode of W–O, bending mode of W–O, and the deformation mode of W–O–W, respectively, were observed (see Fig. 6c) similar to those found in the good crystalline WO_3 samples (25, 26), showing the occurrence of the crystallization. Meanwhile, the amorphous structure of the WO_3/SiO_2 sample after reaction for three times could be regenerated after being treated at 823 K for 6 h since all the peaks disappeared, as shown in Fig. 6b. These results were in good agreement with the aforementioned activity test. A similar Raman spectrum was also obtained when the WO_3/SiO_2 sample was calcined at 973 K, as shown in Fig. 6d.

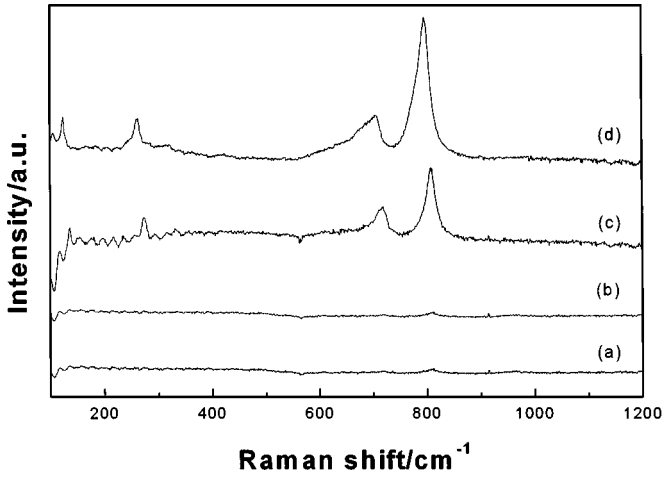

FIG. 6. Raman spectra of the 15% WO_3/SiO_2 sample calcined at 823 K. (a) before reaction, (b) after regeneration, (c) after reaction, and (d) the 15% WO_3/SiO_2 sample calcined at 973 K.

The RDF curves of the anhydrous WO_3 and WO_3/SiO_2 samples obtained from Fourier transforms of their EXAFS $k^2 x$ at the W L_3 edge are shown in Fig. 7. For the anhydrous WO_3, as shown in Fig. 7a, the peaks between R = 0.6~2.5 Å were assigned to W–O bonds and the peaks at R = 3.7 Å to the W–W bonds, respectively (27). RDF curves similar to the WO_3/SiO_2 catalyst after reaction for three times or the WO_3/SiO_2 catalyst after being calcined at 973 K were also obtained. In comparison with that of anhydrous WO_3, a new peak around 3.3 Å appeared on the RDF

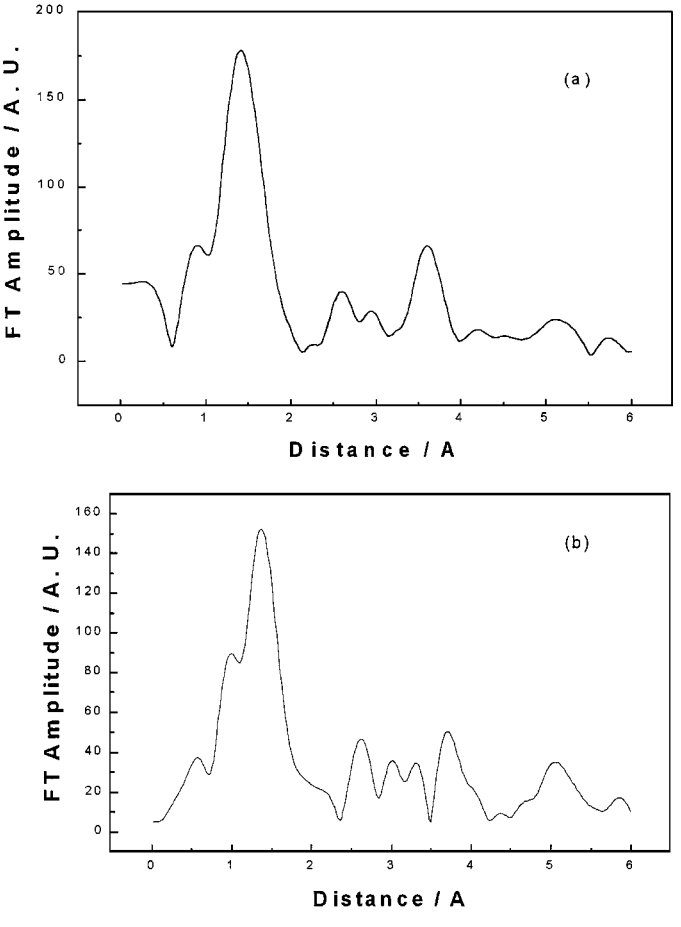

FIG. 7. RDF curves of W k edge in (a) anhydrous WO_3 and (b) 15% WO_3/SiO_2 sample calcined at 823 K.

TABLE 3

Influence of Various Solvents on the Performance of the WO_3/SiO_2 Catalyst with 15 wt% WO_3 Loading[a]

Solvent	Conversion of CPE (%)	Yield of GA (%)
MeOH	93.1	12.1
EtOH	91.5	38.5
i-PrOH	95.7	57.4
t-BuOH	100	59.9
MeCN	74.7	44.4
THF	78.1	47.1

[a] Reaction conditions: 5 ml each of the solvents, other conditions are as the same as those given in Table 1.

curve of WO_3/SiO_2 sample, as shown in Fig. 7b, which was possibly attributed to a W–Si bond resulting from WO_3 anchoring onto the SiO_2 surface. A new shoulder peak around 2.1 Å with a high Debye–Waller factor was presumably corresponding to the W–O bonds in the W–O–W and W–O–Si bridges (28). Such W–O–Si bridges, as confirmed by Raman spectra (29), have been claimed to be favorable for the selective oxidation reaction (30–33). The calculation from the EXAFS data also revealed that the coordination number of W in the above-mentioned bridges was 4.8. Such unsaturated W sites on the surface (25) favored the adsorption of reactants and in turn, increased the catalytic activity of the WO_3/SiO_2 catalyst.

Effect of the Solvents

It is well known that the solvent plays a very important role in determining the catalytic activity and selectivity in many catalytic oxidations by H_2O_2 (34). Therefore, the effects of various common solvents on the catalytic performance of the 15 wt% WO_3/SiO_2 catalyst during the CPE oxidation to GA were investigated. As shown in Table 3, higher conversion and better selectivity to GA were obtained in the tert-butanol (t-BuOH) medium than those in other media, such as methanol, ethanol, iso-propanol, acetonitrile, and tetrahydrofurian. According to the GC-MS analysis, the promoting effect of t-BuOH on the CPE oxidation to GA could be attributed to the formation of tert-butyl hydroperoxide (TBHP) through to the reaction between H_2O_2 and t-BuOH with WO_3/SiO_2 as an acid catalyst (Scheme 2), which has been proved to be an excellent oxidant for the selective CPO to GA in liquid phase (15, 24).

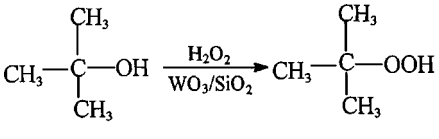

SCHEME 2. Route of TBHP formation.

CONCLUSION

The following conclusions can be drown from this study:

1. The WO_3/SiO_2 catalyst is one of the powerful heterogeneous catalysts for the liquid phase cyclopentene oxidation by H_2O_2, which exhibits high activity and excellent selectivity to GA. The as-prepared catalyst seems more suitable for the industrial process than those homogeneous catalysts owing to the convenience in the separation of the catalyst from the reaction products, which makes it possible to use the catalyst repetitively and to regenerate the deactivated catalyst.

2. In the WO_3/SiO_2 catalyst, the amorphous WO_3 species are determined to be the active sites. The anhydrous WO_3 exhibited almost no activity because of its good crystalline structure. The optimum WO_3 loading is determined as 15 wt% to ensure the largest number of active sites but without significant crystallization. The optimum calcination temperature is determined as 823 K to guarantee the strongest interaction and support under the condition that no significant crystallization occurs, which can effectively inhibit the leaching of the active sites during the reaction. The t-BuOH is proved to be the best solvent in the present oxidation reaction owing to the promoting effect of TBHP formed through the reaction between t-BuOH and H_2O_2 on WO_3/SiO_2 as an acid catalyst.

3. Under the present conditions, the 15 wt% WO_3/SiO_2 catalyst can be used repetitively for three times (72 h). After reaction for 72 h, significant decrease in the activity of WO_3/SiO_2 catalyst was observed, possibly due to the structural conversion of WO_3 from the amorphous state to the crystalline state. The deactivated catalyst could be regenerated easily by calcining it at 823 K for 6 h.

ACKNOWLEDGMENTS

This work was supported by the National Natural Science Foundation of China and SINOPEC. We are also grateful to the Committee of Shanghai Education for providing financial support for this study.

REFERENCES

1. Morikawa, S., Takahashi, K., Mogi, J., and Kurita, S., *Bull. Chem. Soc. Jpn.* **55**, 2254 (1982).
2. Martin, C., Solana, G., Rives, V., Marci, G., Palmisano, L., and Sclafani, A., *Catal. Lett.* **49**, 235 (1997).
3. Kamata, H., Takahashi, K., and Ingemar Odenbrand, C. U., *Catal. Lett.* **53**, 65 (1998).
4. Zhang, Z. Suo, J., Zhang, X., and Li, S., *J. Chem. Soc., Chem. Comm.* 241 (1998).
5. Ishii, Y., Yamawaki, K., Ura, T., Yoshida, H., and Ogana, M., *J. Org. Chem.* **53**, 3587 (1988).
6. Oguchi, M., Ura, T., Ishii, Y., and Ogana, M., *Chem. Lett.* 857 (1989).
7. Karagezyan, G. M., USSR SU Patent 878760, 1981.
8. Daicel Chemical Industries Ltd. Co., JP Patent 59108734, 1984.
9. Gorman, S. P., Scott, E. M., and Russell, A. D., *J. Appl. Bacteriol.* **48**, 161 (1980).

10. Wang, W. J., Qiao, M. H., Li, H. X., and Deng, J.-F., *Appl. Catal. A* **166**, 243 (1998).
11. Wang, W. J., Qiao, M. H., Li, H. X., Dai, W. L., and J.-F., Deng, and Deng, J.-F., *Appl. Catal. A* **168**, 151 (1998).
12. Furakawa, H., Nakamura, T., Inagaki, H., Nishikawa, E., Imai, C., and Misono, M., *Chem. Lett.* 877 (1988).
13. Deng, J.-F., Xu, X. H., Chen, H. Y., and Jiang, A. R., *Tetrahedron* **48**, 3503 (1992).
14. Lee, K.-Y., Itoh, K., Hashimoto, M., Mizuno, N., and Misono, M., *Stud. Surf. Sci. Catal.* **82**, 583 (1994).
15. Hutter, R., Mallat, T., and Baiker, A., *J. Catal.* **153**, 177 (1995).
16. Jin, R., Xia, X., Xue, D., and Deng, J.-F., *Chem. Lett.*, 371 (1999).
17. Yoldas, B. E., *J. Non-Cryst. Solids* **38**, 81 (1980).
18. Aizawa, M., Nosaka, Y., and Fujii, N., *J. Non-Cryst. Solids* **128**, 77 (1991).
19. Dutoit, D. C. M., Schneider, M., and Baiker, A., *J. Catal.* **153**, 165 (1995).
20. Stolarski, M., Walendziewski, J., and Pniak, M. S. B., *Appl. Catal. A* **177**, 139 (1999).
21. Arata, K., *Adv. Catal.* **37**, 165 (1989).
22. Ji, W., Hu, J., and Chen, Y., *Catal. Lett.* **53**, 15 (1998).
23. Vaidyaanathan, N., Houaua, M., and Hercules, D. M., *Catal. Lett.* **43**, 209 (1997).
24. Sheldon, R. A., Wallau, M. I., Arends, W. C. E., and Schuchardt, U., *Acc. Chem. Res.* **31**, 485 (1998).
25. Wachs, I. E., Hardcastle, F. D., and Chan, S. S., *Spectroscopy* **1**, 30 (1986).
26. Vuurman, M. A., and Wachs, I. E., *J. Phys. Chem.* **95**, 9928 (1991).
27. Salje, E., and Rietveld, H. M., *Acta Crystallogr. A* **31**, 356 (1975).
28. Hilbrig, F., Gobel, H. E., Knozinger, H., Schmelz, H., and Lengeler, B., *J. Phys. Chem.* **95**, 6973 (1991).
29. Wachs, I. E., Kim, D. S., and Ostromecki, M., *J. Mol. Catal. A* **106**, 93 (1996).
30. Dadyburjor, D. B., Jewur, S. S., and Ruckenstein, E., *Catal. Rev. Sci. Eng.* **19**, 293 (1979).
31. Haber, J., *in* "New Developments in Selective Oxidation by Heterogeneous Catalysis" (B. Delmon, Ed.), Vol. 72, p. 279. Elsevier, Amsterdam 1992.
32. Kung, H. H., *Ind. Eng. Chem. Prod. Res. Dev.* **25**, 171 (1986).
33. Centi, G., and Trifiro, F., *Appl. Catal.* **12**, 1 (1984).
34. Hulea, V., Dumitriu, E., Patcas, F., Ropot, R., Graffin, P., and Moreau, P., *Appl. Catal. A* **170**, 169 (1998).